



UNIVERSITY OF LEEDS

This is a repository copy of *A beta-sheet interaction interface directs the tetramerisation of the Miz-1 POZ domain*.

White Rose Research Online URL for this paper:
<http://eprints.whiterose.ac.uk/79624/>

Version: Accepted Version

Article:

Stead, MA, Trinh, CH, Garnett, JA et al. (4 more authors) (2007) A beta-sheet interaction interface directs the tetramerisation of the Miz-1 POZ domain. *Journal of Molecular Biology*, 373 (4). 820 - 826. ISSN 0022-2836

<https://doi.org/10.1016/j.jmb.2007.08.026>

Reuse

Unless indicated otherwise, fulltext items are protected by copyright with all rights reserved. The copyright exception in section 29 of the Copyright, Designs and Patents Act 1988 allows the making of a single copy solely for the purpose of non-commercial research or private study within the limits of fair dealing. The publisher or other rights-holder may allow further reproduction and re-use of this version - refer to the White Rose Research Online record for this item. Where records identify the publisher as the copyright holder, users can verify any specific terms of use on the publisher's website.

Takedown

If you consider content in White Rose Research Online to be in breach of UK law, please notify us by emailing eprints@whiterose.ac.uk including the URL of the record and the reason for the withdrawal request.



eprints@whiterose.ac.uk
<https://eprints.whiterose.ac.uk/>

A Beta-Sheet Interaction Interface Directs Tetramerisation of the Miz-1 POZ Domain

Mark A Stead¹, Chi H Trinh², James A Garnett^{2,3}, Stephen B Carr², Andrew J Baron², Thomas A Edwards²
and Stephanie C Wright^{1*}

¹Molecular Cell Biology Research Group and ²Astbury Centre for Structural Molecular Biology,
Garstang/Astbury Buildings, Institute of Molecular and Cellular Biology,
Faculty of Biological Sciences, University of Leeds, Leeds LS2 9JT

³Present address:

Division of Molecular Biosciences
Imperial College London
South Kensington Campus
London SW7 2AZ

*corresponding author

s.c.wright@leeds.ac.uk

tel: +44 0113 343 3133

fax +44 0113 343 3167

Running Title: Crystal Structure of the Miz-1 POZ domain

SUMMARY

The POZ/BTB domain is an evolutionarily conserved motif found in approximately forty zinc-finger transcription factors (POZ-ZF factors). Several POZ-ZF factors are implicated in human cancer, and POZ-domain interaction interfaces represent an attractive target for therapeutic intervention. Miz-1 is a POZ-ZF factor that regulates DNA-damage-induced cell cycle arrest, and plays an important role in human cancer by virtue of its interaction with the c-Myc and Bcl6 oncogene products. The Miz-1 POZ domain mediates both self-association and the recruitment of non-POZ partners. POZ-ZF factors generally function as homo-dimers, although higher-order associations and heteromeric interactions are known to be physiologically important; crucially, the interaction interfaces in such large complexes have not been characterised. We report here the crystal structure of the Miz-1 POZ domain to 2.1Å resolution. The tetrameric organisation of Miz-1 POZ reveals two types of interaction interface between subunits; an interface of alpha-helices resembles the dimerisation interface of reported POZ domain structures, whereas a novel beta-sheet interface directs the association of two POZ domain dimers. We show that the beta-sheet interface directs tetramerisation of the Miz-1 POZ domain in solution, and therefore represents a newly described candidate interface for the higher-order homo- and hetero-oligomerisation of POZ-ZF proteins *in vivo*.

Keywords:

BCL6

BTB domain

c-Myc

The POZ/BTB (*p*oxvirus and *z*inc finger/*b*ric-à-brac, *t*ramtrack and *b*road complex) domain mediates protein-protein interactions in diverse biological processes, and is found in approximately forty zinc finger transcription factors (POZ-ZF factors)¹. Most POZ-ZF factors play roles in cell proliferation and development, and many have also been implicated as oncogenes or tumour suppressors in human cancer²; structural analysis of POZ domains will ultimately aid the design of cancer therapies that target POZ-ZF function³.

Miz-1 (*M*yc-*i*nteracting *z*inc finger protein⁴) is a POZ-ZF factor that activates genes involved in cell cycle arrest, differentiation and DNA damage responses. The transcriptional properties of Miz-1 are modulated by binding of the c-myc proto-oncogene product to residues near its zinc-finger domain, leading to aberrant gene regulation in tumours. Many biological activities of Miz-1 are mediated by its N-terminal POZ domain, which directs both self-association and the recruitment of non-POZ partners. POZ-ZF proteins are generally considered to function as biological homodimers via a POZ-POZ interaction; crystal structures of three POZ-ZF POZ domains, PLZF (*p*romyelocytic *l*eukaemia *z*inc *f*inger)^{5 6}, BCL6 (*B* *c*ell *l*ymphoma *6*)⁷ and LRF (*l*eukaemia/lymphoma *r*elated *f*actor)^{8 9} reveal tightly intertwined dimers with an extensive hydrophobic interface. Different POZ domains recruit specific non-POZ partners, thereby conferring distinct biological properties on the various POZ-ZF factors. Miz-1 is regulated during DNA damage responses by the recruitment of TOPBP1 (*t*opoisomeraseII *b*inding *p*rotein)¹⁰, and its interaction with the ubiquitin ligase, HECTH9 (*h*omologous to *E*6-AP *c*arboxy-*t*erminus)¹¹, modulates the ubiquitination and therefore transcriptional properties of c-Myc.

Higher-order oligomers¹² and heteromeric interactions¹³ between different POZ-ZF factors are thought to be physiologically important, although the interaction interfaces in these complexes have not been characterised. We report here the crystal structure of the tetrameric Miz-1 POZ domain. The oligomeric organisation of Miz-1 POZ reveals a novel beta-sheet interaction interface that directs the association of two POZ domain dimers. We show that this region mediates the association of Miz-1 POZ dimers in solution, and therefore represents a newly described candidate interface for the higher-order homo- and hetero-oligomerisation of POZ-ZF proteins *in vivo*.

General Organisation of the Miz-1 POZ Domain

The entire Miz-1 POZ domain (Miz-1 residues 2 – 115) was expressed in *E.coli*, purified and crystallized. The crystal structure was solved by molecular replacement and refined to $R = 18.1\%$, $R_{\text{free}} = 22.9\%$ at 2.1 Å resolution (Table 1 and Figure 1A), with a single tetramer per asymmetric unit. All residues were built in the model.

The Miz-1 POZ tetramer may be described as an association of two dimers, each of which resembles the reported PLZF, BCL6 and LRF POZ structures (Figure 1). The assembly has two distinct types of interface between subunits: the A:B and C:D interfaces resemble those described in PLZF, BCL6 and LRF, whereas A:D and B:C are novel; this tetrameric organisation of POZ-ZF POZ domains has not been observed previously. Estimates of the chemical stability of assemblies in the crystal lattice (http://www.ebi.ac.uk/msd-srv/prot_int/pistart.html¹⁴) suggest that the Miz-POZ tetramer represents a stable physiological association that dissociates into dimers specifically across the A:D and B:C interfaces. The AB and CD dimers are predicted to be stable, in agreement with reports that POZ-ZF POZ domains are obligate homodimers¹⁵. In contrast, dissociation of the tetramer across the A:B and C:D interfaces is not expected to occur, as the resulting AD and BC dimers are predicted to be unstable. The buried surface areas are 1244 Å² per monomer for the A:B and C:D interfaces, and 754 Å² per monomer for A:D and B:C. We refer to A:B and C:D as the Miz-1 POZ domain dimerisation interfaces, and A:D and B:C as tetramerisation interfaces.

The Miz-1 POZ Domain Core and Dimerisation Interface

POZ domains of the POZ-ZF factors are highly conserved, and a sequence alignment of Miz-1 with PLZF, BCL6 and LRF reveals identities of 33%, 36% and 40% respectively (Figure 2A). The PLZF, BCL6 and LRF POZ domains each comprise 6 alpha-helices and 5 beta-strands, with a central core of alpha-helices being flanked at the top and bottom by short beta-sheets (described according to orientation of the BCL6 dimer shown in Figure 1A). Notably, Miz-1 lacks residues that form the β1 strand of PLZF, BCL6 and LRF; the organisation of secondary structure elements is otherwise identical, and we used the same nomenclature for their designation.

The overall organisation of the Miz-1 POZ domain core is the same as PLZF, BCL6 and LRF (Figure 1B); compared to Miz-1, the RMSD values of Cα atom positions for monomers are 2.64 Å (PLZF), 2.36 Å (BCL6), and 2.22 Å (LRF). The α5 and α6 helices are in a slightly different position in Miz-1 compared with the

reported POZ domains, being rotated outwards away from the core of the molecule. The positioning of [$\alpha 5$ plus $\alpha 6$] in BCL6, PLZF and LRF may be stabilised by interactions between $\alpha 6$ and $\beta 1'$ in these structures. The C-chain $\alpha 6$ helix was somewhat disordered in our model, with relatively high B factors and poor electron density in this region. The corresponding residues were well ordered in all other chains, and we therefore modelled this region using superposition of chain A. These features of the C chain $\alpha 6$ helix probably reflect a lack of crystal contacts involving these residues in comparison to chains A, B and D. Notably, the elongin POZ domain lacks an $\alpha 6$ helix, and the position of $\alpha 6$ in other POZ-ZF POZ domains is more variable than the other secondary structure elements, suggesting that this region does not play a critical role in stabilisation of the POZ monomer core.

The organisation of the Miz-1 POZ dimerisation interface differs from PLZF, BCL6 and LRF due to the absence of the $\beta 1$ strand (Figure 1). The interfaces of PLZF, BCL6 and LRF have previously defined distinct regions: a hydrophobic interface of alpha-helices at the centre of the structure is formed by the close packing of $\alpha 1$, $\alpha 2$ and $\alpha 3$ from each subunit, whereas two beta-sheet interfaces at the bottom are formed by the interaction of $\beta 1$ of one chain with $\beta 5$ from its partner ($\beta 1$ - $\beta 5'$; Figure 1A box). The lower beta-sheet interaction interface, which accounts for 40-50% of the surface area buried upon dimerisation of the PLZF, BCL6 and LRF POZ domains, is notably absent in Miz-1. Although the $\beta 1$ - $\beta 5'$ sheet cannot form in Miz-1, $\beta 5$ residues are found in the same location in all four structures. The A:B and C:D interfaces of Miz-1 POZ resemble the central region of the PLZF, BCL6 and LRF dimerisation interfaces, although the $\alpha 1$ helix is slightly longer in Miz-1. The buried surface area in the Miz-1 A:B and C:D interfaces is lower than the overall dimerisation interface of other POZ domains (values are 1244 \AA^2 per monomer for Miz-1, 1928 \AA^2 for PLZF [PDB 1buo], 1706 \AA^2 for BCL6 [PDB 1r28] and 1621 \AA^2 for LRF [PDB 2nn2]), but higher than the isolated central interfaces of these structures; these differences reflect the lack of $\beta 1$ and longer $\alpha 1$ region in Miz-1. Importantly, the natural absence of an N-terminal $\beta 1$ strand does not prevent dimerisation of the Miz-1 POZ domain.

Tetramerisation of the Miz-1 POZ Domain

Tetramerisation of the Miz-1 POZ domain results from the association of two dimers at solvent-exposed beta-sheets, $\beta 3$ - $\beta 2$ - $\beta 4$, located at the top of each monomeric subunit. This interaction leads to the displacement of an outer $\beta 4$ strand from one of the subunits of each constituent dimer, generating a tetramer with two

5-stranded beta-sheet interaction interfaces organised $\beta 3^A$ - $\beta 2^A$ - $\beta 4^D$ - $\beta 2^D$ - $\beta 3^D$ and $\beta 3^B$ - $\beta 2^B$ - $\beta 4^B$ - $\beta 2^C$ - $\beta 3^C$ (Figures 1A and 2B); the two displaced $\beta 4$ strands adopt an alpha helical conformation, and lie parallel to $\alpha 5$ on one face of the tetramer (Figures 1A and 2B, helix α^A). The rearrangement of secondary structure elements is frequently observed in protein interactions involving beta-sheets, and the conversion of $\beta 4$ to α during tetramerisation of the Miz-1 POZ domain may be facilitated by the flexibility of the loop between $\alpha 3$ and $\beta 4$. This displacement of $\beta 4$ leads to loss of the original symmetry axis of the POZ dimer; the two-fold rotation axis of the Miz-1 POZ tetramer is perpendicular to its largest face, and extends through a hole in its centre. The tetramerisation interface is stabilised mainly by beta-sheet interactions, and by a salt bridge between Asp58^{B/D} at the N-terminus of $\beta 4$ and Lys39 at the N-terminus of $\alpha 2^{A/C}$. The organisation of the Miz-1 POZ tetramer is unlike the POZ/T1 domain tetramer of the potassium ion channels; these latter structures have polar interaction interfaces, with the tetramer subunits being arranged around a 4-fold symmetry axis running through a central pore in the ion channel ¹⁶.

Tetramerisation of POZ-ZF POZ domains has not been reported previously; although POZ dimers have been observed to interact via their lower $\beta 1$ - $\beta 5'$ sheets in some crystal lattices (for example, ⁶), this interaction has not been confirmed in solution, and may be due to crystal packing. We therefore determined the oligomeric state of the Miz-1 POZ domain in solution by analytical ultracentrifugation. Both velocity and equilibrium centrifugation indicated that the protein was in a dynamic tetramer-dimer equilibrium with a Kd of approximately 110 μ M (data presented in the Supplementary Information). In order to confirm the role of the beta-sheet interface in POZ domain tetramerisation, we mutated the outer $\beta 4$ strand to a sequence not expected to form stable interactions internally within beta-sheets ¹⁷; the Miz-1 POZ $\beta 4$ strand was shortened by one residue, and a centrally located valine mutated to an aspartate residue (V60D; Δ 61mutant; Figure 2C). This mutant POZ domain sedimented solely as a dimer when analysed by analytical ultracentrifugation (data presented in the Supplementary Information), suggesting that the $\beta 4$ strand is critical for tetramer formation.

Surface Features of the Miz-1 POZ Domain

Surface features of the POZ-ZF POZ domains should determine interactions with specific non-POZ partners. For example, BCL6 recruits the SMRT (silencing mediator for retinoid and thyroid hormone receptors) transcriptional co-repressor to lateral grooves (Figure 1A) that extend from the dimer interface across the

bottom of the molecule⁷. A charged pocket that lies at the top between the dimer subunits (Figure 1A) has also been implicated in co-repressor recruitment in PLZF and BCL6; the depth of this pocket and its surrounding charge differ between various POZ domains. Since the Miz-1 POZ domain exists in a dimer-tetramer equilibrium, its potential interaction surfaces change according to oligomeric state. Notably, tetramerisation blocks access to the charged pocket (D25; K39); although these residues are conserved in Miz-1, no function has been ascribed to this region and there is no evidence that the Miz-1 POZ domain recruits co-repressors. The two faces of the Miz-1 POZ tetramer are non-identical, with the two α helices that form during tetramerisation being exposed on the same side. The bottom of the Miz-1 dimer is less concave than the reported POZ domains and has a marked protrusion in its centre; this reflects the absence of β 1, the rotation of α 6, and the longer α 1 regions in Miz-1. The overall surface charge distribution of the Miz-1 POZ tetramer is non-uniform (Figure 3). Both large faces have an overall neutral charge, whereas the sides are strikingly acidic. The charge distribution on the bottom surfaces of the various POZ domain dimers is very different, consistent with the role of the lateral groove in the recruitment of specific non-POZ partners (Figure 3).

Implications

The novel cross-dimer beta-sheet interaction interface of the Miz-1 POZ tetramer mediates a dynamic, reversible association of POZ domain dimers. The biological activity of the POZ-ZF factors may be modulated by specific hetero-oligomerisation, although crucially the stoichiometry of such complexes has not been rigorously analysed; it will now be pertinent to determine whether the beta-sheet interaction interface described here may be used to modulate Miz-1 function via the formation of combinatorial hetero-tetramers with other POZ-ZF proteins. Although homo-tetramers have not been reported in other POZ-ZF factors, it is possible that they may use the β 3- β 2- β 4 interface to direct the formation of hetero-tetramers. Interaction interfaces are used to direct specific combinatorial patterns of homo- and hetero-oligomerisation in many other systems: for example, in the Myc/Mad/Max transcription factor network, the helix-loop-helix leucine zipper region of Max mediates both homo- and hetero-dimer formation, whereas the Myc and Mad proteins use this same region solely for hetero-dimerisation¹⁸. Interestingly, the T1/POZ domain of the potassium channels directs ion channel diversity via the formation of specific heterotetramers; it will be relevant to determine whether the POZ domain plays a similar role in determining the specificity of hetero-oligomer formation in the POZ-ZF factors.

ACKNOWLEDGEMENTS

This work was funded by Yorkshire Cancer Research, the Wellcome Trust under the Joint Infrastructure Fund (JIF) initiative, and a Marie Curie International Reintegration Grant. We thank staff at the SRS (Daresbury UK) for assistance with X-ray data collection, and Simon Phillips for comments on the manuscript.

ACCESSION NUMBER

The coordinates and structure factors have been deposited with the PDB with the ID code of 2Q81.

ACCEPTED MANUSCRIPT

LEGENDS TO FIGURES

Figure 1**Structure of the Miz-1 POZ Domain****(A) Ribbon representation of the Miz-1 POZ domain tetramer**

Subunits A, B, C and D are indicated in different colours. Secondary structure elements of the A chain and of the A:D interface are shown. The structure of the BCL6 POZ domain (PDB 1r28) is shown for comparison; the box indicates the $\beta 1$ - $\beta 5'$ beta-sheet of the BCL6 dimerisation interface that is absent in Miz-1 (positions on the partner chain of BCL6 are indicated with primes).

The Miz-1 POZ domain (residues 2 - 115) was expressed as a GST-fusion protein in *E.coli* BL21(DE3)pLysS. The GST tag was removed by cleavage with PreScission protease, and the Miz-1 POZ domain fragment purified by chromatography on Q sepharose, Resource Q and Supadex 75. Crystals of the purified Miz-1 POZ domain were obtained by hanging drop vapour diffusion against 20% PEG 3350, 20% PEG 400, 200 mM $MgCl_2$, 100 mM HEPES pH 7.5. Details of plasmid construction, protein purification, X-ray data collection and structure determination are reported in the Supplementary Information.

(B) Superposition of POZ domain C α atoms for Miz-1, BCL6, PLZF and LRF.

Stereo image of superpositions of POZ domain dimers (PDBs: BCL6 1r28; PLZF 1buo; LRF 2nn2; the Miz-1 dimer corresponds to chains A and B). Miz-1 (green), BCL6 (cyan), LRF (magenta), PLZF (yellow).

Figure 2**Organisation of the Miz-1 POZ domain tetramerisation interface****(A) Sequence alignment of the Miz-1, PLZF, BCL6 and LRF POZ domains**

Sequences were aligned using ClustalW. The observed secondary structure of the Miz-1 POZ chains is indicated: alpha helices (yellow); beta sheets (red); residues that have different conformations in individual chains of the tetramer (blue). $\beta 5$ (pink) is conserved between the POZ domains, but does not form part of a beta-sheet in Miz-1. The N-terminal residues of PLZF, BCL6 and LRF (boxed) encode the $\beta 1$ strand that is absent from the Miz-1 POZ domain.

(B) Structure of the Miz-1 tetramer beta-sheet interface

Secondary structure elements are coloured as in the sequence alignment in (A).

(C) Mutation of the Miz-1 POZ domain beta-sheet interface

The sequence of the Miz-1 POZ domain β 4 strand mutant [V60D; Δ 61] is indicated. Side chains of the D chain β 4 strand residues are indicated; positions 60 and 61 are shown in magenta and green respectively. Analytical ultracentrifugation of wild-type and mutant Miz-1 POZ domains is reported in the Supplementary Information.

Figure 3**Electrostatic Surface Representation of the Miz-1 POZ domain**

Both flat faces of the Miz-1 POZ tetramer are shown together with bottom and side surfaces; the bottom surfaces of the BCL6, PLZF and LRF POZ dimers are shown for comparison.

TABLE 1

Data collection and refinement statistics

Crystal parameters

Space group	C 2 2 2 ₁
Cell dimensions	a = 65.54, b = 128.52, c = 116.04

Data collection

Resolution (Å)	64.26 - 2.10
Wavelength (Å)	0.98
R_{merge} (%)	5.2 (30)
$I/\sigma I$	21.7 (6.1)
Number unique reflections	28,911
Multiplicity	6.1 (6.1)
Completeness (%)	99.8 (100)

Refinement

Resolution (Å)	2.1
R (%)	18.1
R_{free} (%)	22.9
RMSD stereochemistry	
Bond lengths (Å)	0.011
Bond angles (°)	1.179
Number of protein atoms	3,588
Number of water molecules	239
Average B factor	27.833
Ramachandran analysis (%)	
Most favoured	91.8
Additionally allowed	8.0
Generously allowed	0.2
Disallowed	0

$R_{merge} = \sum |I - \langle I \rangle| / \sum I$ where I is the integrated intensity of a given reflection and $\langle I \rangle$ is the mean intensity of multiple corresponding symmetry-related reflections.

$R = \sum ||F_o| - |F_c|| / \sum F_o$ where F_o and F_c are the observed and calculated structure factors respectively.

$R_{free} = R$ calculated using 5% random data excluded from the refinement.

Numbers in parentheses correspond to the highest resolution shell of 2.1 - 2.21 Å.

RMSD stereochemistry is the deviation from ideal values.

Ramachandran analysis was carried out using PROCHECK¹⁹.

REFERENCES

1. Stogios, P. J., Downs, G. S., Jauhal, J. J., Nandra, S. K. & Prive, G. G. (2005). Sequence and structural analysis of BTB domain proteins. *Genome Biol* **6**, R82.
2. Kelly, K. F. & Daniel, J. M. (2006). POZ for effect--POZ-ZF transcription factors in cancer and development. *Trends Cell Biol* **16**, 578-87.
3. Polo, J. M., Dell'Oso, T., Ranuncolo, S. M., Cerchietti, L., Beck, D., Da Silva, G. F., Prive, G. G., Licht, J. D. & Melnick, A. (2004). Specific peptide interference reveals BCL6 transcriptional and oncogenic mechanisms in B-cell lymphoma cells. *Nat Med* **10**, 1329-35.
4. Peukert, K., Staller, P., Schneider, A., Carmichael, G., Hanel, F. & Eilers, M. (1997). An alternative pathway for gene regulation by Myc. *Embo J* **16**, 5672-86.
5. Li, X., Peng, H., Schultz, D. C., Lopez-Guisa, J. M., Rauscher, F. J., 3rd & Marmorstein, R. (1999). Structure-function studies of the BTB/POZ transcriptional repression domain from the promyelocytic leukemia zinc finger oncoprotein. *Cancer Res* **59**, 5275-82.
6. Ahmad, K. F., Engel, C. K. & Prive, G. G. (1998). Crystal structure of the BTB domain from PLZF. *Proc Natl Acad Sci U S A* **95**, 12123-8.
7. Ahmad, K. F., Melnick, A., Lax, S., Bouchard, D., Liu, J., Kiang, C. L., Mayer, S., Takahashi, S., Licht, J. D. & Prive, G. G. (2003). Mechanism of SMRT corepressor recruitment by the BCL6 BTB domain. *Mol Cell* **12**, 1551-64.
8. Schubot, F. D., Tropea, J. E. & Waugh, D. S. (2006). Structure of the POZ domain of human LRF, a master regulator of oncogenesis. *Biochem Biophys Res Commun* **351**, 1-6.
9. Stogios, P. J., Chen, L. & Prive, G. G. (2007). Crystal structure of the BTB domain from the LRF/ZBTB7 transcriptional regulator. *Protein Sci* **16**, 336-42.
10. Herold, S., Wanzel, M., Beuger, V., Frohme, C., Beul, D., Hillukkala, T., Syvaaja, J., Saluz, H. P., Haanel, F. & Eilers, M. (2002). Negative regulation of the mammalian UV response by Myc through association with Miz-1. *Mol Cell* **10**, 509-21.
11. Adhikary, S., Marinoni, F., Hock, A., Hulleman, E., Popov, N., Beier, R., Bernard, S., Quarto, M., Capra, M., Goettig, S., Kogel, U., Scheffner, M., Helin, K. & Eilers, M. (2005). The ubiquitin ligase HectH9 regulates transcriptional activation by Myc and is essential for tumor cell proliferation. *Cell* **123**, 409-21.

12. Katsani, K. R., Hajibagheri, M. A. & Verrijzer, C. P. (1999). Co-operative DNA binding by GAGA transcription factor requires the conserved BTB/POZ domain and reorganizes promoter topology. *Embo J* **18**, 698-708.
13. Kobayashi, A., Yamagiwa, H., Hoshino, H., Muto, A., Sato, K., Morita, M., Hayashi, N., Yamamoto, M. & Igarashi, K. (2000). A combinatorial code for gene expression generated by transcription factor Bach2 and MAZR (MAZ-related factor) through the BTB/POZ domain. *Mol Cell Biol* **20**, 1733-46.
14. Krissinel, E. & Henrick, K. (2005). *Detection of protein assemblies in crystals*. Lecture notes in computer science, 3695/2005, Springer Berlin/Heidelberg.
15. Li, X., Lopez-Guisa, J. M., Ninan, N., Weiner, E. J., Rauscher, F. J., 3rd & Marmorstein, R. (1997). Overexpression, purification, characterization, and crystallization of the BTB/POZ domain from the PLZF oncoprotein. *J Biol Chem* **272**, 27324-9.
16. Kreusch, A., Pfaffinger, P. J., Stevens, C. F. & Choe, S. (1998). Crystal structure of the tetramerization domain of the Shaker potassium channel. *Nature* **392**, 945-8.
17. Hoskins, J., Lovell, S. & Blundell, T. L. (2006). An algorithm for predicting protein-protein interaction sites: Abnormally exposed amino acid residues and secondary structure elements. *Protein Sci* **15**, 1017-29.
18. Grandori, C., Cowley, S. M., James, L. P. & Eisenman, R. N. (2000). The Myc/Max/Mad network and the transcriptional control of cell behavior. *Annu Rev Cell Dev Biol* **16**, 653-99.
19. Laskowski, R. A., MacArthur, M. W., Moss, D. S. & Thornton, J. M. (1993). PROCHECK: a program to check the stereochemical quality of protein structures. *Journal of Applied Crystallography* **26**, 283-291.
20. CCP4. (1994). The CCP4 suite: programs for protein crystallography. *Acta Crystallogr D Biol Crystallogr* **50**, 760-3.
21. Keegan, R. M. & Winn, M. D. (2007). Automated search-model discovery and preparation for structure solution by molecular replacement. *Acta Crystallogr D Biol Crystallogr* **63**, 447-57.
22. McCoy, A. J., Grosse-Kunstleve, R. W., Storoni, L. C. & Read, R. J. (2005). Likelihood-enhanced fast translation functions. *Acta Crystallogr D Biol Crystallogr* **61**, 458-64.
23. Perrakis, A., Morris, R. & Lamzin, V. S. (1999). Automated protein model building combined with iterative structure refinement. *Nat Struct Biol* **6**, 458-63.
24. Emsley, P. & Cowtan, K. (2004). Coot: model-building tools for molecular graphics. *Acta Crystallogr D Biol Crystallogr* **60**, 2126-32.

25. Murshudov, G. N., Vagin, A. A. & Dodson, E. J. (1997). Refinement of macromolecular structures by the maximum-likelihood method. *Acta Crystallogr D Biol Crystallogr* **53**, 240-55.
26. Maiti, R., Van Domselaar, G. H., Zhang, H. & Wishart, D. S. (2004). SuperPose: a simple server for sophisticated structural superposition. *Nucleic Acids Res* **32**, W590-4.
27. DeLano, W. L. (2002). *The PyMOL molecular graphics system*, DeLano Scientific, Palo Alto, CA, USA.
28. Schuck, P. (2000). Size-distribution analysis of macromolecules by sedimentation velocity ultracentrifugation and lamm equation modeling. *Biophys J* **78**, 1606-19.
29. Stafford, W. F. & Sherwood, P. J. (2004). Analysis of heterologous interacting systems by sedimentation velocity: curve fitting algorithms for estimation of sedimentation coefficients, equilibrium and kinetic constants. *Biophys Chem* **108**, 231-43.

TABLE 1

Data collection and refinement statistics

Crystal parameters

Space group	C 2 2 2 ₁
Cell dimensions	a = 65.54, b = 128.52, c = 116.04

Data collection

Resolution (Å)	64.26 - 2.10
Wavelength (Å)	0.98
R_{merge} (%)	5.2 (30)
$I/\sigma I$	21.7 (6.1)
Number unique reflections	28,911
Multiplicity	6.1 (6.1)
Completeness (%)	99.8 (100)

Refinement

Resolution (Å)	2.1
R (%)	18.1
R_{free} (%)	22.9
RMSD stereochemistry	
Bond lengths (Å)	0.011
Bond angles (°)	1.179
Number of protein atoms	3,588
Number of water molecules	239
Average B factor	27.833
Ramachandran analysis (%)	
Most favoured	91.8
Additionally allowed	8.0
Generously allowed	0.2
Disallowed	0

$R_{merge} = \sum |I - \langle I \rangle| / \sum I$ where I is the integrated intensity of a given reflection and $\langle I \rangle$ is the mean intensity of multiple corresponding symmetry-related reflections.

$R = \sum ||F_o| - |F_c|| / \sum F_o$ where F_o and F_c are the observed and calculated structure factors respectively.

$R_{free} = R$ calculated using 5% random data excluded from the refinement.

Numbers in parentheses correspond to the highest resolution shell of 2.1 - 2.21 Å.

RMSD stereochemistry is the deviation from ideal values.

Ramachandran analysis was carried out using PROCHECK¹⁹.

FIGURE 1

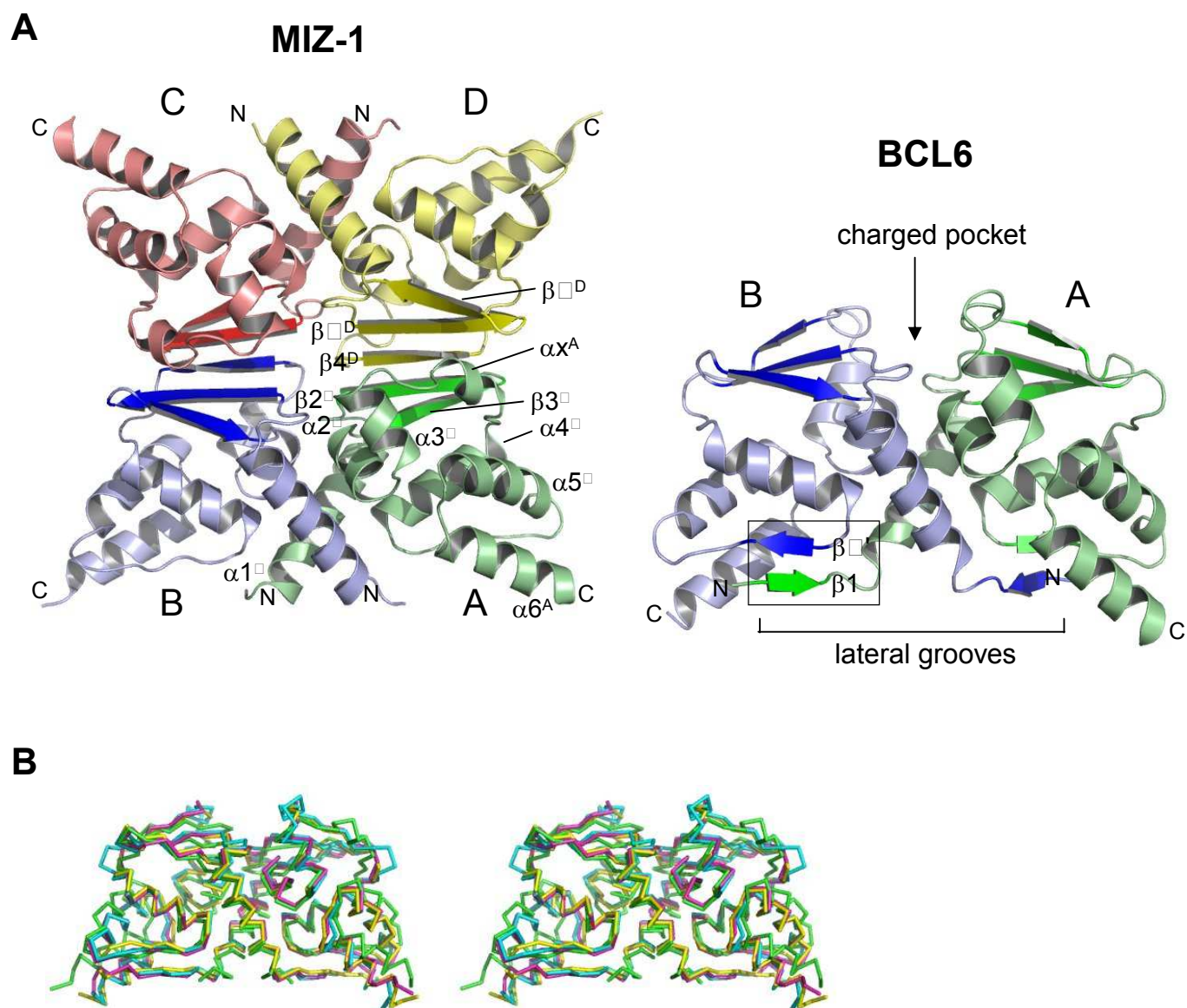


FIGURE 2

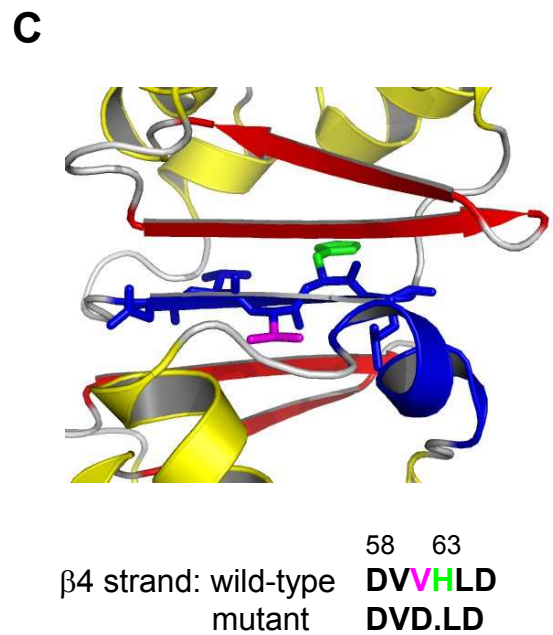
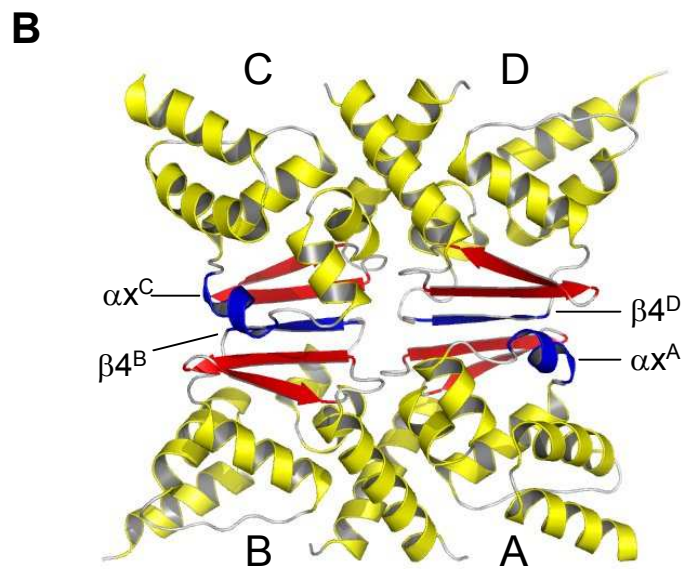
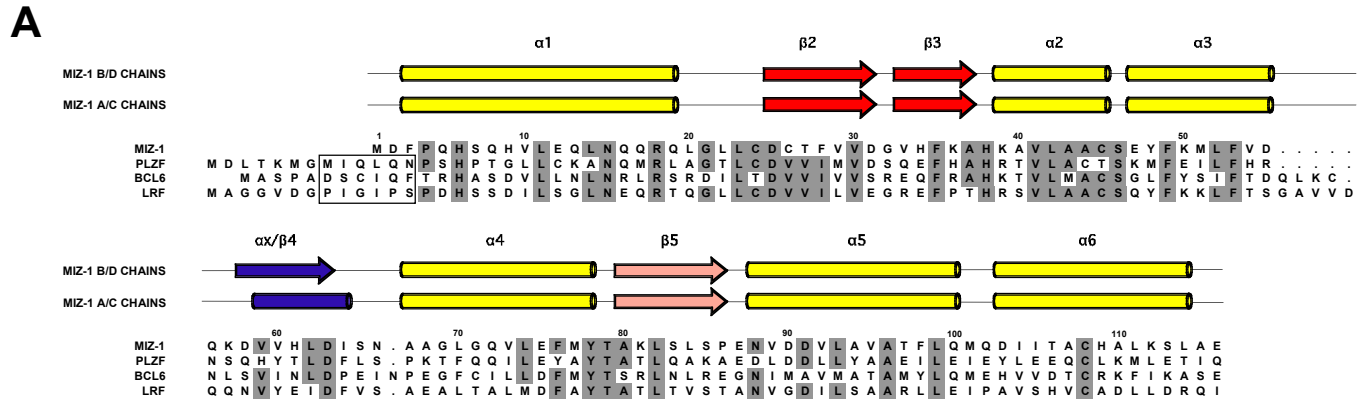


FIGURE 3

